Pis'ma v ZhETF, vol. 85, iss. 4, pp. 251 – 254 

# FCC/BCC competition and enhancement of saturation magnetization in nanocrystalline Co-Ni-Fe films

*N. G. Chechenin*[1)], *E. V. Khomenko, J. Th. M. de Hosson*[+]

*Skobeltsyn Institute of Nuclear Physics, Lomonosow Moscow State University, 119992 Moscow, Russia*

[+]*Materials Science Center, University of Groningen, NL 9747 AG Groningen,The Netherlands*

Submitted 26 December 2006

Resubmitted 22 January 2007

Structure, chemical composition and magnetic properties of electrochemically deposited nanocrystalline Co-Ni-Fe films were investigated by a number of techniques. A high saturation magnetic induction up to $B_s = 21$ kG was attained. An enhancement of saturation magnetization, compared to an ideal anticipated one was revealed, which correlated with the nonlinear behavior of structural phase composition and lattice parameters with the change of the composition.

PACS: 75.75.+a, 75.37.Nq

Soft magnetic thin films with high magnetic moment are used in various applications, such as magnetic recording systems, high frequency planar inductors and modern nonvolatile magnetic memory. Currently, such a widespread ferromagnetic substance is permalloy. However, ternary Co-Ni-Fe alloy possesses much higher saturation magnetization [1]. Moreover, competition among *fcc* and *bcc* crystalline phases decreases coercive force and magnetostriction. At the same time, a complicated correlation between deposition condition, microstructure and magnetic properties is a basic constraint of an industrial application of this material. In this paper we analyze saturation magnetization, structure and lattice parameters of the electrodeposited thin Co-Fe-Ni films as a function of chemical composition.

Nanocrystalline CoNiFe films were prepared by the electrochemical method on

Cu(250 nm)/Cr(25 nm)/$SiO_2$(300 nm)/Si-substrate.

Uniaxial magnetic anisotropy was obtained applying a permanent magnetic field around of 800 Oe oriented along the substrate surface during the film deposition. Details of the film deposition can be found in [2].

The chemical composition of the films was determined by the energy dispersive analysis of X-rays (SEM-EDS and TEM-EDS). The concentration of Co, Fe and Ni varied between 0.30 to 0.54, 0.12 to 0.31, and 0.15 to 0.58, respectively. From X-ray diffraction (XRD) study we have learned that the CoNiFe films are normally composed of the *fcc* and *bcc* competing structural phases, as illustrated in Fig.1. More experimental details of investigation of microstructure and composition have been reported previously in our publications [2 – 4] as well as in earlier works [1, 5]. In particular, it has been established that the films were higly textured with the (111) XRD-line dominating for the *fcc* crystallites and (110) XRD-line for *bcc* crystallites and this kind of the texture was kept even after annealing [3]. Due to this fact the two lines were normally used for estimations of the *fcc*-to-*bcc* fractions in the films. In present work, the *fcc*-fraction and *bcc*-fraction present in the alloy were obtained from areas under the $(111)_{fcc}$, $A_{fcc}$, and $(110)_{bcc}$, $A_{bcc}$, XRD lines, respectively. From the XRD line widths we estimated that the grain size for the *fcc* phase was about 30 nm for most of the samples, while it was about 10 to 20 nm for *bcc* grains. The saturation magnetization $I_S$ as well as the anisotropy field $H_k$ were obtained from ferromagnetic resonance (FMR)

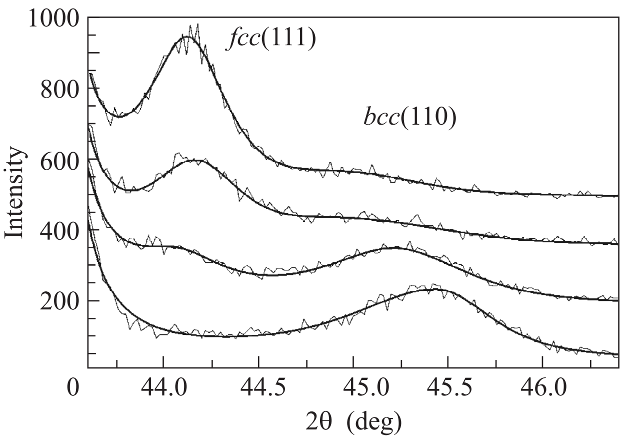


Fig.1. XRD spectra of Co-Fe-Ni films. Smooth lines are fitted curves

[1)]Corresponding author. Tel.: +7-495-9392348; fax: +7-495-939-08-96; e-mail: chechenin@sinp.msu.ru

measurements at the frequency $f = 9.40\,\mathrm{GHz}$ in an external magnetic field range up to 5 kOe aligned along the film surface, comparing the resonance fields along easy (EA) and hard (HA) axes and applying the Kittel relationships:

$$\omega^2 = \gamma^2(H_R^{EA} + H_k)(H_R^{EA} + H_k + 4\pi I_s) \qquad (1a)$$

$$\omega^2 = \gamma^2(H_R^{HA} - H_k)(H_R^{HA} - H_k + 4\pi I_s), \qquad (1b)$$

where $\omega = 2\pi f$ is the frequency of the applied RF-field, $\gamma$ is the gyromagnetic ratio, $H_R^{EA}$ and $H_R^{HA}$ are resonance values of the DC-field applied in the EA and HA directions, respectively. Typical FMR spectra are demonstrated in Fig.2 and more experimental details of

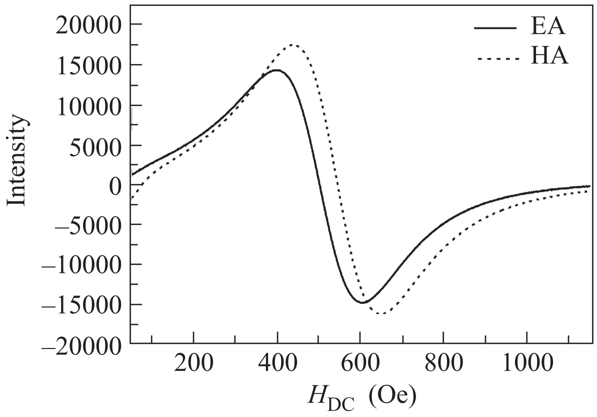


Fig.2. FMR spectra for EA and HA directions of the applied magnetic field

the FMR investigation have been reported in [2]. Depending on the composition, the saturation magnetic induction varied between $4\pi I_s = 16.7$ and 21 kG, which is a high value, compared to that of permalloy.

The variation of the chemical composition has a strong influence on the structure as well as on the magnetic properties [1–5]. To study the effect of the composition in a generalized way we combine here the two independent parameter of the composition of the ternary alloy into a single number of electrons per atom:

$$n_e = 27x + 28y + 26z,$$

where $x$, $y$ and $z$ are the concentrations of Co, Ni and Fe in the alloy, respectively, with $x + y + z = 1$.

Fig.3 shows the natural logarithm of the $A_{fcc}/A_{bcc}$ ratio as a function of the number of electrons per atom $n_e$ in the Co-Ni-Fe alloy. The dashed line is the line of the equal population of the $fcc$ and $bcc$ phases. A quite pronounced peak of $\ln(A_{fcc}/A_{bcc})$ is seen at around $n_e = 27.0$, evidencing a dominance of the $fcc$-phase.

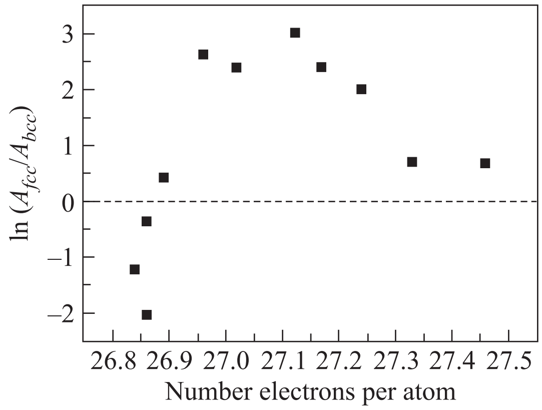


Fig.3. The ratio of the $fcc$- and $bcc$-fractions as a function of the number of electrons per atom $n_e$

Increase of $n_e$ above this value, i.e. decrease of Fe content, leads a surprising decrease of the $fcc$ fraction and to a parity of the two phases. A reduction of $n_e$ below 27.0, i.e. an increase of Fe content leads to a single $bcc$ phase structure which is the natural structure for the $\alpha$-Fe.

From the positions of the $(111)_{fcc}$ and $(110)_{bcc}$ XRD lines the lattice parameters $a_{\rm exp}^{fcc}$ and $a_{\rm exp}^{bcc}$ were obtained which varied also with chemical composition. In a simplest ideal case the lattice parameter of a random binary alloy can follow the linear Vegard law [6], if the pure components have the same type of the lattice. For a ternary alloy with different structure of pure components (pure Co and Ni crystals have $fcc$ while pure Fe preferably has the $bcc$ structure) the experimental lattice parameter can be compared with a concentration weighted combination, based on atomic volumes per atom, as suggested by Zen [7]. Assuming that in both, the $fcc$ and the $bcc$ phase, the volume per atom is the same and taking into account that there are two atoms in the $bcc$ and four atoms in the $fcc$ lattices, we write for ideal lattice parameters:

$$a_{ideal}^{fcc} = a_{\rm Co}^{fcc}x + a_{\rm Ni}^{fcc}y + \sqrt[3]{2}a_{\rm Fe}^{bcc}z, \qquad (2a)$$

$$a_{\rm ideal}^{bcc} = \frac{1}{\sqrt[3]{2}}(a_{\rm Co}^{fcc}x + a_{\rm Ni}^{fcc}y) + a_{\rm Fe}^{bcc}z. \qquad (2b)$$

The ratios $a_{\rm exp}^{fcc}/a_{\rm ideal}^{fcc}$ and $a_{\rm exp}^{bcc}/a_{\rm ideal}^{bcc}$ of the experimental lattice parameters to the ideal anticipated ones as a function of composition in terms of number of electron per atom $n_e$ are plotted in Fig.4. The lattice parameters of $fcc$-Co, $fcc$-Ni and $bcc$-Fe are equal to 3.544 Å, 3.515 Å and 2.867 Å, respectively. The volume required per single atom in Fe is about 5.9% larger than that per Co and about 8.5% larger than that per Ni atoms. Therefore, the largest change of the alloy lattice parameter occurs when the concentration of Fe varies. Largest

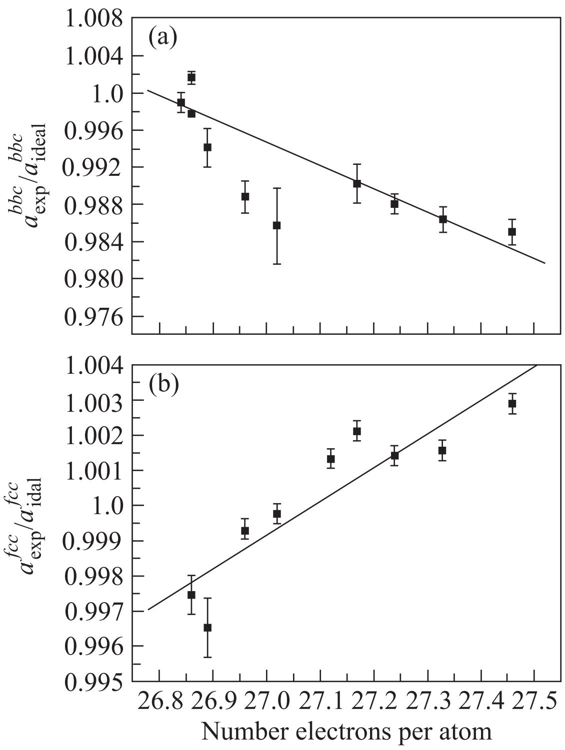


Fig.4. Ratios of the experimental lattice parameters to the ideal anticipated versus predicted by Eqs.(2) for the $bcc$ (a) and $fcc$ (b) structural phases. Solid line is a linear fit to the data

values of $a_{ideal}^{fcc}$ and $a_{ideal}^{bcc}$ equal to 3.61 Å and 2.867 Å, respectively, correspond to a dominance of Fe in the alloy.

The deviation of the ratios from the unity can be interpreted as a nonlinear deformation of the crystal lattice cells. When Fe concentration decreases, i.e. $n_e$ increases, the $a_{\rm exp}^{bcc}$ lattice parameter decreases faster (Fig.4a) than predicted by Eq.(2b). In the $fcc$ phase the lattice parameter $a_{\rm exp}^{fcc}$ is larger than what follows from Eq.(3a), so the ratio $a_{\rm exp}^{fcc}/a_{\rm ideal}^{fcc}$ is larger than unity at small concentration of Fe (large value of $n_e$). However it falls down below unity at larger iron concentration (smaller value of $n_e$), Fig.4b. One can also note a sharp decrease of $a_{\rm exp}^{bcc}$ around $n_e = 27.0$, i.e. in the region of peak of $\ln(A_{fcc}/A_{bcc})$. It could be qualitatively interpreted as a strong contraction of the $bcc$ nanosize grains due to an interface mismatch effect of dominating $fcc$ grains boundaries. The $fcc$ grains experience a size expansion in the same region due to a similar mismatch effect from the neighboring $bcc$ grain boundaries, as can be seen in Fig.4b.

Similar to the ideal lattice parameters, one can compose an ideal anticipated saturation magnetization $I_S^a$ of Co-Ni-Fe alloy as a linear combination of partial magnetizations

$$I_S^a = I_S^{\rm Co}x + I_S^{\rm Ni}y + I_S^{\rm Fe}z, \qquad (3)$$

where the partial magnetic moments $I_S^x$ of pure $fcc$-Co, $fcc$-Ni and $bcc$-Fe are 1400, 480 and 1700 G, respectively. With such a representation we can expect a variation of $4\pi I_S^a$ in the range of 11 to 17 kG for the variation of the composition in the investigated films. The observed $4\pi I_S^{\rm obs}$ values diverge systematically from the anticipated values.

One can see from Fig.5, that while the ratio $I_S^{\rm obs}/I_S^a$ is close to one at low $n_e \approx 26.8$, it tends to increase

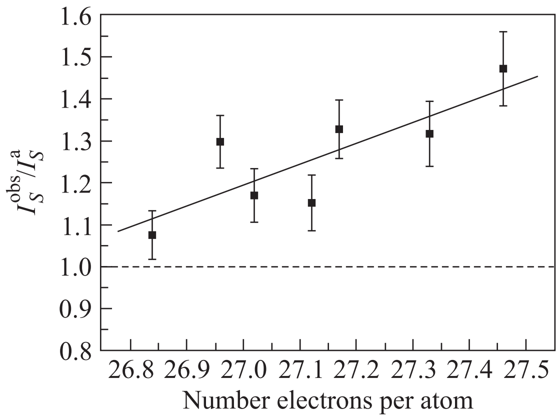


Fig.5. Enhancement of the saturation magnetization. Solid line is a linear fit to the data

at high $n_e$ values. Most of the experimental points are positioned above the dashed line, which levels the observed and anticipated values. It is evident from the graph, that the observed saturation magnetization shows a kind of enhancement compared with the ideal anticipated values, especially for lower iron concentration or higher number of electrons per atom. In other words, the data show a kind of tendency to slow down the decrease of the magnetic moment with decrease of iron concentration.

A deviation from the Vegard law or from the Zen law for binary system is a common observation and there is no reason why these deviations could diminish in a ternary alloy. Evidently, this kind of nonlinear deformation is connected with a complicated rearrangement of the outer shell electron configurations in a disordered alloy. For the case of competing nanocrystalline structural phases, the interface mismatch causes a nonlinear deformations which also induce an additional reconfiguration of the outer shell electrons. However, comparing the data, we can conclude that the internal (change in composition) and the external (interface effect) induced electron reconfigurations have a different influence on magnetic properties of the alloy. While systematic nonlinearity, i.e. a general decrease of $a_{\rm exp}^{bcc}/a_{\rm ideal}^{bcc}$ and increase of $a_{\rm exp}^{fcc}/a_{\rm ideal}^{fcc}$ with increase of $n_e$ correlate with a systematic behavior of $I_S^{\rm obs}/I_S^a$, there is no a clear evidence of a strong effect of interface effect on $I_S^{\rm obs}/I_S^a$, which definitely presents in the lattice parameter behavior. Moreover, from comparison of Fig.3 and Fig.5 we can conclude that the enhancement of $I_S^{\rm obs}/I_S^a$ is more evident when the parity of the competing phases stabilizes.

The work is carried out in the framework of the Agreement on scientific cooperation between SINP MSU and Department of Materials Science, RUG and partially supported by the grant NSh-5365.2006.2 of the President of Russian Federation.

---

1. T. Osaka, M. Takai, K. Hayashi et al., Nature **392**, 796 (1998).
2. E. V. Khomenko, S. N. Polyakov, N. G. Chechenin, and E. E. Shalyguina, Adv. Materials (in Russian) **2**, 66 (2006).
3. E. H. du Marchie van Voorthuysen, F. T. tem Broek, N. G. Chechenin, and D. O. Boerma, J. Magn. Magn. Mater. **266**, 251 (2003).
4. N. G. Chechenin, E. H. du Marchie van Voorthuysen, J. Th. M. De Hosson, and D. O. Boerma, J. Magn. Magn. Mater. **290-291**, 1539 (2005).
5. X. Liu, G. Zangari, and L. Shen, J. Appl. Phys. **87**, 5410 (2000).
6. L. Vegard, Z. Phys. **5**, 17 (1921).
7. E-an Zen, Amer. Mineralogist **41**, 523 (1956).